

Deformation Heterogeneity Study of a 6061-T6 Aluminum Alloy Processed by Equal Channel Angular Pressing

Reyes-Ruiz C.^{1,2,a}, Figueroa I.A.^{1,b}, Braham C.^{2,c}, Cabrera J.M.^{3,4,d},
Zanellato O.^{2,e}, Baiz S.^{2,f} and Gonzalez G.^{1,2,g}

¹Instituto de Investigaciones en Materiales, Universidad Nacional Autónoma de México, Circuito exterior S/N, Cd. Universitaria, A.P. 70-360, Coyoacán, C.P. 04510, Mexico

²Laboratoire Procédés et Ingénierie Mécanique et Matériaux, CNRS UMR 8006, ENSAM-CNAM, 151, Bd de l'Hôpital 75013, Paris, France

³Departamento de Ciencia de los Materiales e Ingeniería Metalúrgica, ETSEIB-Universidad Politécnica de Cataluña, Av Diagonal 647, 08028 Barcelona, Spain

⁴Fundació CTM Centre Tecnològic, Pl. de la Ciencia 2, 08243-Manresa, Spain.

^ac.reyesruiz@comunidad.unam.mx, ^biafigueroa@unam.mx, ^cchedly.braham@ensam.eu,
^djose.maria.cabrera@upc.edu, ^eolivier.zanellato@cnam.fr, ^fsarah.baiz@cnam.fr,
^gjoseggr@unam.mx

Keywords: AA6061-T6, ECAP, Synchrotron, Residual Stress, Diffraction

Abstract. Among the severe plastic deformation techniques, the equal channel angular pressing (ECAP) has drastically improved the mechanical properties of the processed alloys. However, information regarding friction phenomenon, which modifies the deformation at the surface and the heterogeneity microstrain state produced by the process itself, is still scarce. In the present work, the deformation heterogeneity and the friction effect, at the surface in the bulk material of the 6061-T6 aluminum alloy processed by ECAP, is presented and discussed. The residual stress (RS) measurements were performed by means of X-Ray diffraction. By means of synchrotron diffraction, volumetric sections of the ECAPed samples were characterized. Finite element analysis showed a good agreement with the experimentally obtained residual stress and microhardness mapping results. The study also showed that the highest deformation zones were located at the outer parts of the deformed samples (top and bottom), while the inner zone showed strain oscillations of up to 49 ± 2 MPa.

Introduction

The possibility of achieving ultrafine grain (UFG) microstructure in polycrystalline materials in solid state has been achieved through the severe plastic deformation (SPD) processes. Among these processes, equal channel angular pressing (ECAP) is one of the preferred techniques for grain refinement. At present, there is a well-defined idea about the mechanisms for grain refinement, generation of substructures and their macroscopic influence over the fatigue life, yield stress, UTS, ductility, etc. [1,2] Subgrain misorientation, low angle boundaries transformation (LAGB) into high angle grain boundaries (HAGB), dislocation multiplication and annihilation and texture evolution are the main contributors of the mechanisms for grain refinement and substructures generation of the highly deformed alloys [3,4].

For a number of engineering applications, mechanical and structural proprieties i.e. microstructure homogeneity and hardness are very important. Therefore, several studies on ECAP for aluminum (Al) and Al-alloys have been reported [5-7].

With the help of finite element analysis, the design of the die set can be evaluated. The results of such analysis can determine the geometry that could provide the lowest inhomogeneity coefficient, preserving a good relationship with a high shear deformation [8,9]. Besides, the determination of the residual stress state, in the vicinity of the die walls and the core of the sample, is highly pertinent [10-12], as the friction effects significantly change the microdeformations.

Based on this, the objective of the present investigation was to evaluate the deformation variation and the residual stress distribution in the ECAPed samples, including the surface and central part, using high energy synchrotron radiation and conventional XRD. The experimental results were also compared to the finite element analysis (FEA).

Experimental

A 6061-T6 aluminum alloy with 1.0%Mg, 0.6%Si, 0.7%Fe, 0.25%Cu, 0.15%Mn, 0.2%Cr, 0.25%Zn and 0.15Ti% (in wt. %) was used for this study. The T6 condition was chosen in order to avoid a post-ECAP heat treatment. Several bars were cut in samples of 60 X10 mm (length and diameter). Just one ECAP pass was performed at room temperature, using a homemade steel die-set (Fig. 1). The geometrical configuration of the die-set had an outer angle $\psi=37^\circ$ and intersection angle of $\phi=90^\circ$, with an applied strain rate of 0.5 s^{-1} . MoS_2 compound was used as lubricant.

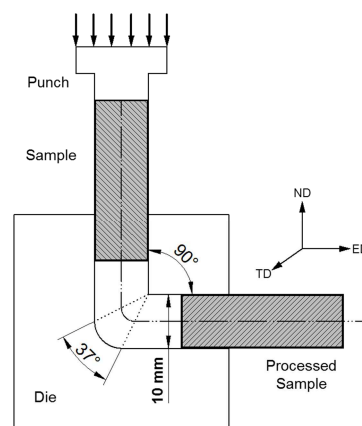


Fig. 1. Experimental setup of the ECAP die-set.

By means of a Proto iXRD diffractometer, the distribution of residual stresses, near the surface, was measured every 30° along the sample circumference (Fig. 2a). The measured peak (422) was obtained with a Cu tube, fitted with a Gaussian profile. It is important to point out that a collimator with an aperture of 2 mm in diameter was used. Ten ψ angles distributed within $\psi = \pm 25^\circ$ were measured, with a $\beta = \pm 3^\circ$ oscillation. The measurements were obtained with an instrumental geometry parallel to extrusion direction (ED).

After electropolishing the ECAP processed samples down to $200 \mu\text{m}$, the in-depth analysis was performed. High energy X-ray diffraction was used, as it has the capacity of measuring volume-average lattice strain in bulk polycrystalline materials, [13]. At the European Synchrotron Radiation Facility (ESRF), the Synchrotron X-Ray diffraction experiments were performed on beamline ID15B. Standard transmission configuration, i.e. a monochromatic 87 keV beam (wavelength $=0.1425 \text{ \AA}$), having a size of $0.5 \times 0.5 \text{ mm}^2$, was employed to carry out the diffraction experiments [14].

The sample was positioned accordingly to Fig. 2b, with the incident beam perpendicular to the normal (ND) and extrusion (ED) directions. Along the normal direction (ND), from -5 mm to +5 mm with a displacement step of 0.5 mm, the diffraction patterns were captured. By means of a 2D detector (MAR 345, marXperts GmbH, 22844 Norderstedt / Germany) with a pixel size of $150 \times 150 \mu\text{m}^2$, placed at a distance of 1277.85 mm from the center of the sample, the Debye-Scherrer rings were obtained. The experimental information or data points were analyzed by FIT2D [15] and the experimental d-spacing were calculated using the values between the opposite points in the diffraction rings.

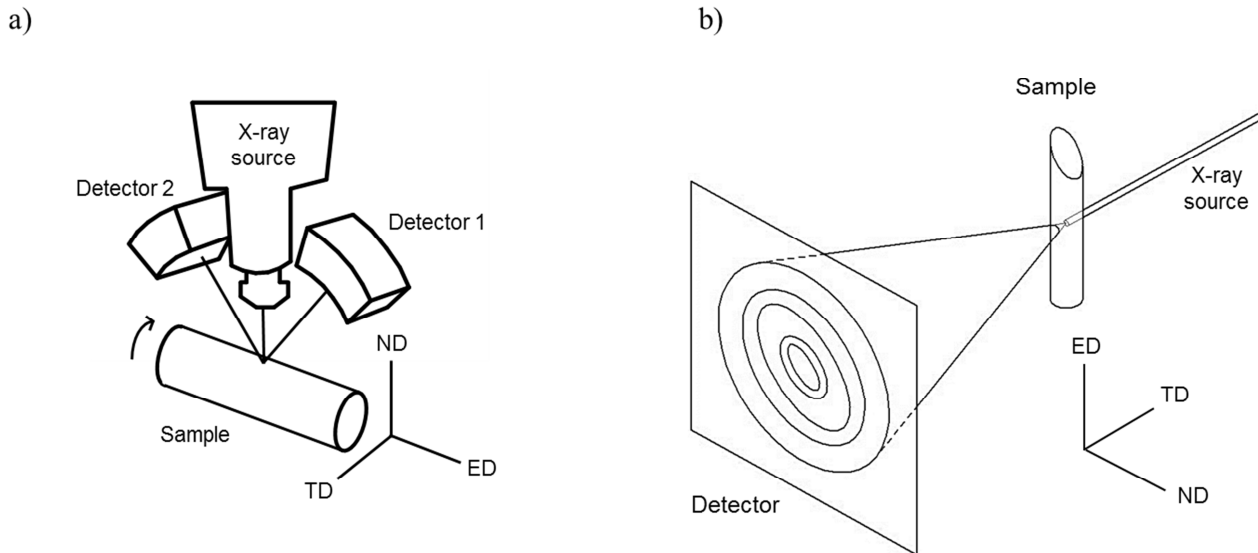


Fig. 2. a) Proto and b) synchrotron experimental setup.

The microhardness was taken using an MMT-X7A Matsuzawa equipment. The indentations were carried out parallel to the extrusion direction (ED), having a 0.5 mm square grid with a load of 100 g for 10 s. By means of a commercially available finite element code “SIMULIA Abaqus®” [16], a three-dimensional finite elements analysis was developed in order to compare and correlate the results obtained from the different techniques used in this study. The ECAP was simulated using a die set channel similar to the one already introduced in this section.

For the three-dimensional finite element analysis, the die set channel was assumed to be discrete rigid (R3D4) and the punch analytically rigid. The billet was modeled considering 3D stress analysis with eight-node linear hexagonal elements (C3D8R). In order to prevent any possible failure of the mesh due to severe deformations, and to reduce the computational time, mass scaling and adaptive meshing were used for all simulations.

The global conditions given to the treated sample at the numerical analysis were the elasto-plastic behavior and strain hardening, having the strain rate and temperature independent. In order to simulate the contact effects at the die-sample interaction, a standard Coulomb friction model was considered, i.e. $\mu=0.1$ [17]. Finally, a lubricated process using MoS_2 compound was assumed.

Results and Discussion

Fig. 3a shows the plot of the results of the microhardness analysis. As expected from the die geometry, a hardness gradient along the normal direction (ND) was found. It is clear that a heterogeneous deformation in the cross-section of the Al bar is produced during the first ECAP pass. The values of the microhardness range from 104 HV to 124 HV, where the highest and lowest values are located at the top and bottom parts of the hardness map, respectively. Approximately 20% was the variation of the experimentally obtained hardness values, being consistent with the results reported in reference [18]. Fig. 3b displays the plastic equivalent deformation (PEEQ) predicted by FEA model. These results are in good agreement with the hardness mapping. It is worthy to mention that the Iwashashi et al.[19] formula, which calculated $\epsilon=1$ for the geometry used in this study, in the first ECAP pass, is only valid for the central zone the ECAPed sample.

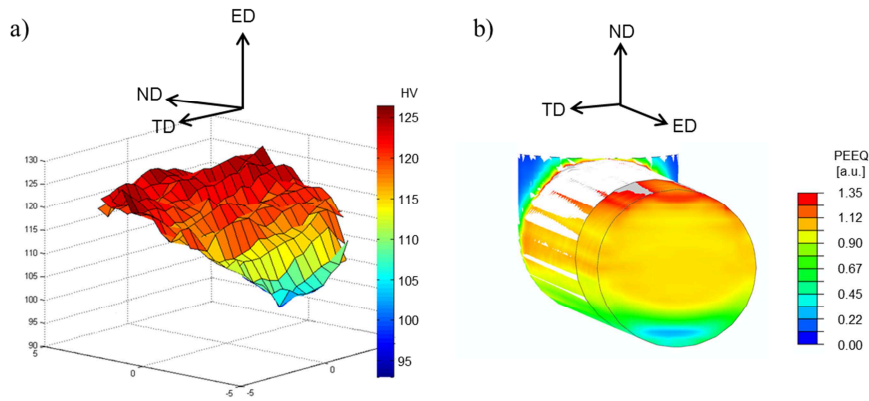


Fig. 3. a) Hardness mapping and b) Equivalent plastic deformation estimated by finite element analysis for the cross-section of the deformed Al sample.

The profile for the surface residual stress was taken along the extrusion direction ($ED=\sigma_{11}$), as shown in Fig. 4. This displayed oscillating values between -50 and -250 MPa. Nevertheless, at in-depth measurement, it was found a propensity to be less compressive. Above 100MPa, such stress variation should be considered significant, particularly with Al alloys. The results of the FEA simulations of the surface stress behavior and the obtained experimental data showed a good agreement. The difference could be attributed to the crystalline texture and grain size; such factors were not included into the numerical model.

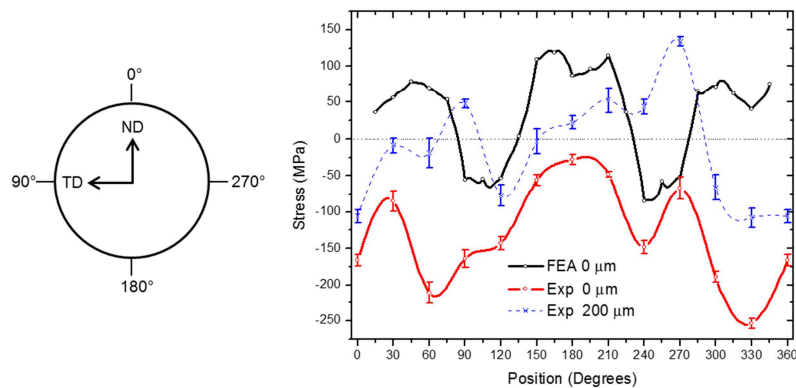


Fig. 4. Surface residual stress (σ_{11}) distribution measured and calculated by FEA.

It was observed that the middle region of the deformed sample has a symmetrical behavior between σ_{11} and σ_{22} , being explained in terms of an isotropic hypothesis, taking the mean value of the stresses obtained for 6 different (hkl) planes: (111), (200), (220), (311), (222) and (331). Besides, the main role of the compressive residual stress distribution for σ_{11} (ED) and tensile for σ_{22} (TD), were clearly observed. It is important to note that effect of the stress oscillations (around 40 MPa) was considered not that critical, however it can no be taken as negligible. The values at the outer sides of the ECAPed Al samples, i.e. between ± 4 and ± 5 mm, showed a complex behavior that was the result of the deformation process and the friction effects convolution. Because of the cylindrical geometry of the sample, the analyzed irradiated volume at the surface of the Al ECAPed samples is relatively small, when compared to the central position (Fig 5), being drawn as dotted lines.

Therefore, at the initial stages of the ECAP process, the generation of a heterogeneous deformation was rather evident. Moreover, with the addition of the friction effects and the aforementioned heterogeneous deformation, the resulting residual stress distribution tended to be very complex. Taking into account the residual stress at the outer part of the deformed sample, the lowest compressive values took place between 150° and 210° (outer angle of the die). This result concurred with three-dimensional finite elements analysis developed for this work.

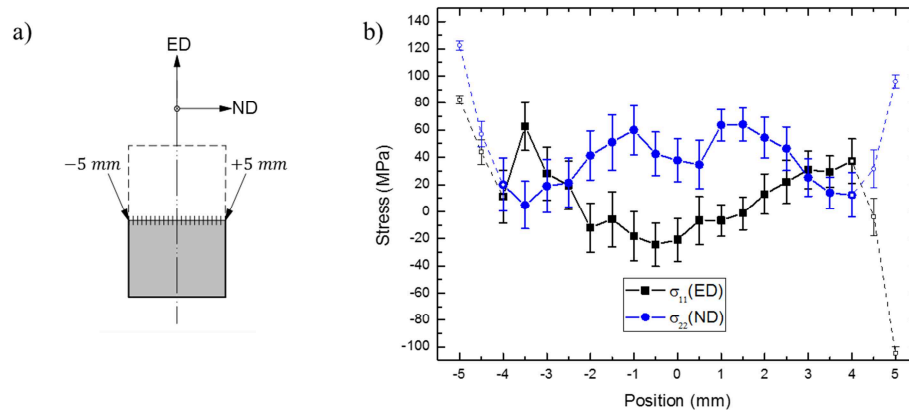


Fig. 5. a) Position of the sample and b) Results of the residual stress obtained in the central zone of the highly deformed Al sample (σ_{11} and σ_{22}).

Conclusion

It was found that the largest value for residual stress distribution was found at the surface of the ECAPed sample, with important oscillations along the circumference of the sample. A plausible explanation for this distribution was given in terms of the ECAP deformation process, which is thought to be pure shear deformation in the bulk, in addition to the contribution of the convolution of the friction effects. Significant variations of up to 50 MPa were observed within the central zone of the studied Al sample. Depending on the considered direction (σ_{11} or σ_{22}), these variations could be either of tensile or compressive nature. The residual stress results of the numerical model and experimental measurements showed a good agreement. The hardness mapping and the calculated plastic deformation distribution displayed an analogous deformation gradient. Further investigation in terms of the evolution of the residual stress and (hkl) anisotropy, as a function of the depth, is highly pertinent.

Acknowledgments

The authors thank the European Synchrotron Radiation Facility (ESRF) for providing the beam time. C. Reyes-Ruiz and G. Gonzalez acknowledge the financial support from CONACYT and PAPIIT through projects No. 166896 and IN110014 and CONACYT scholarship No. 240249. This research was carried out during the sabbatical year of GG at ENSAM-CNAM with the support of PASPA-UNAM and CONACYT. Part of the equipment used in this research was purchased with project UNAM-DGAPA-PAPIIT 101016. Finally, J.M. Cabrera thanks the financial support through project MAT2014-59419-C3-1-R.

References

- [1] R. Z. Valiev and T. G. Langdon, Principles of equal-channel angular pressing as a processing tool for grain refinement, *Prog. Mater. Sci.*, 51 (2006) 881–981.
- [2] C. Reyes-Ruiz, I. A. Figueroa, C. Braham, J. M. Cabrera, I. Alfonso, and G. Gonzalez, Texture and lattice distortion study of an Al-6061-T6 alloy produced by ECAP, *Mater. Trans.* Article in press.
- [3] M. A. Meyers, A. Mishra, and D. J. Benson, Mechanical properties of nanocrystalline materials, *Prog. Mater. Sci.*, 51 (2006) 427–556.
- [4] G. Gonzalez, C. Braham, J. L. Lebrun, Y. Chastel, W. Seiler, and I. A. Figueroa, Microstructure and Texture of Al 2Si x Sn (x = 0 , 4 , 8 mass %) Alloys Processed by Equal Channel Angular Pressing, *Mater. Trans.*, 53 (2012) 1234–1239.

- [5] S. N. Alhajeri, N. Gao, and T. G. Langdon, Hardness homogeneity on longitudinal and transverse sections of an aluminum alloy processed by ECAP, *Mater. Sci. Eng. A*, 528, (2011) 3833–3840.
- [6] A. P. Zhilyaev, D. L. Swisher, K. Oh-ishi, T. G. Langdon, and T. R. McNelley, Microtexture and microstructure evolution during processing of pure aluminum by repetitive ECAP, *Mater. Sci. Eng. A*, 429 (2006) 137–148.
- [7] C. Hernandez, I. A. Figueroa, I. Alfonso, C. Braham, P. Castillo, and G. Gonzalez, Microstructure and texture evolution of the Al-20Sn alloy processed by equal-channel angular pressing using route C, *Mater. Trans.*, 56 (2015) 40–45.
- [8] F. Djavanroodi, B. Omranpour, M. Ebrahimi, and M. Sedighi, Designing of ECAP parameters based on strain distribution uniformity, *Prog. Nat. Sci. Mater. Int.*, 22 (2012) 452–460.
- [9] S. K. Lu, H. Y. Liu, L. Yu, Y. L. Jiang, and J. H. Su, 3D FEM simulations for the homogeneity of plastic deformation in aluminum alloy HS6061-T6 during ECAP, *Procedia Eng.*, 12 (2011) 35–40.
- [10] F. Cioffi, J. I. Hidalgo, R. Fernández, T. Pirling, B. Fernández, D. Gesto, I. Puente Orench, P. Rey, and G. González-Doncel, Analysis of the unstressed lattice spacing, d_0 , for the determination of the residual stress in a friction stir welded plate of an age-hardenable aluminum alloy - Use of equilibrium conditions and a genetic algorithm, *Acta Mater.*, 74 (2014) 189–199.
- [11] M. Mahmoodi, M. Sedighi, and D. a. Tanner, Investigation of through thickness residual stress distribution in equal channel angular rolled Al 5083 alloy by layer removal technique and X-ray diffraction, *Mater. Des.*, 40 (2012) 516–520.
- [12] I.-F. Lee, T. Q. Phan, L. E. Levine, J. Z. Tischler, P. T. Geantil, Y. Huang, T. G. Langdon, and M. E. Kassner, Using X-ray microbeam diffraction to study the long-range internal stresses in aluminum processed by ECAP, *Acta Mater.*, 61(2013) 7741–7748.
- [13] A. Wanner and D. C. Dunand, Synchrotron X-ray study of bulk lattice strains in externally loaded Cu-Mo composites, *Metall. Mater. Trans. A*, 31 (2000) 2949–2962.
- [14] J. Romero, M. Preuss, and J. Quinta da Fonseca, Capturing the texture changes in a zirconium alloy during the allotropic phase transformation, *Scr. Mater.*, 61 (2009) 399–402.
- [15] A. P. Hammersley, S. O. Svensson, M. Hanfland, a. N. Fitch, and D. Hausermann, Two-dimensional detector software: From real detector to idealised image or two-theta scan, *High Press. Res.*, 14 (1996) 235–248.
- [16] ABAQUS Inc., ABAQUS 6.9 Analysis User's Manual.
- [17] E. Cerri, P. P. De Marco, and P. Leo, FEM and metallurgical analysis of modified 6082 aluminium alloys processed by multipass ECAP: Influence of material properties and different process settings on induced plastic strain, *J. Mater. Process. Technol.*, 209 (2009) 1550–1564.
- [18] C. Xu, M. Furukawa, Z. Horita, and T. G. Langdon, The evolution of homogeneity and grain refinement during equal-channel angular pressing: A model for grain refinement in ECAP, *Mater. Sci. Eng. A*, 398 (2005) 66–76.
- [19] Y. Iwahashi, J. Wang, Z. Horita, M. Nemoto, and T. G. Langdon, Principle of equal-channel angular pressing for the processing of ultra-fine grained materials, *Scr. Mater.*, 35 (1996) 143–146.